

Investigation of hydrological time series using copulas for detecting catchment characteristics and anthropogenic impacts

Takayuki Sugimoto¹, András Bárdossy^{1,2}, ~~and~~ Geoffrey G. S. Pegram² ~~and~~ Johannes Cullmann³

¹ Institute for Modelling Hydraulic and Environmental Systems, University of Stuttgart, Stuttgart, Germany

² Civil Engineering Program, University of KwaZulu-Natal, Durban, South Africa

~~³ Federal Institute of Hydrology, Koblenz, Germany~~

³ Water & Climate Department, World Meteorological Organization, Geneva, Switzerland

Abstract. Global climate change can have impacts on characteristics of rainfall-runoff events and subsequently on the hydrological regime. Meanwhile, the catchment itself changes due to anthropogenic influences. However, it is not easy to prove the link between the hydrology and the forcings. In this context, it ~~mightean~~ be meaningful to detect the temporal changes of catchments independent from climate change by investigating existing long term discharge records. For this purpose, a new stochastic system based on copulas for time series analysis is introduced. While widely used time series models are based on linear combinations of correlations assuming a Gaussian behavior of variables, a statistical tool like the copula has the advantage to scrutinize the dependence structure of the data in the uniform domain independent of the marginal.

Two measures in the copula domain are introduced herein:

1. Copula asymmetry is defined for copulas and calculated for discharges; this measure describes the non symmetric property of the dependence structure and differs from one catchment to another due to the intrinsic nature of both runoff and catchment.

2. Copula distance is defined as Cramér-von Mises type distance calculated between two copula densities of different time scales. This measure describes the variability and

Style Definition: MTDisplayEquation

Formatted: Font: 12 pt, Bold

interdependency of dependence structures similar to variance and covariance, which can assist in identifying the catchment changes.

These measures are calculated for 100 years of daily discharges for the Rhine rivers and tributaries. Comparing the results of copula asymmetry and copula distance between an Antecedent Precipitation Index—(API)—and simulated discharge time series by a hydrological model we ~~can~~ show the interesting signals of systematic modifications along the Rhine rivers in the last 30 years.

Keywords : Catchment discharge characteristics, Copula stochastic analysis, API, Model uncertainty

1. Introduction

In order to understand the water cycle behavior of a region, it is important to determine its characteristics, but this is difficult to achieve due to the diversity of the system response at different time and space scales. In particular, temporal variability makes parameter estimation difficult and the assessment of model uncertainty essential. As a part of the endeavor to understand ~~grasp~~ the hydrological system, the objective of this research, assessing the anthropogenic impacts on the catchment characteristic independent of the climate change, is therefore important, yet hard to accomplish.

The first possible approach is to statistically test the existence or change of trend in hydrological time series which can be related to climate changes or anthropogenic impacts. Mann-Kendall's Test was performed to confirm the existence of a trend in the annual discharge, precipitation and sediment loads, then ~~and discussed~~ the human intervention and climate impacts based on the available information of the catchments were discussed (Wu et al., 2012). Pettitt's Method (Pettitt, 1979) can be used to detect the time point of trend alternation and analyze the impacts based on a double mass curve (Gao et al., 2012) or a hydrological model

48 (Karlsson et al., 2014). These non-parametric methods for detecting the signal seem, however, not capable
49 enough of explaining when and how much the system had changed, thus making it still difficult to relate the
50 change ~~due to~~ human activities.

51 On the other hand, runoff events are initiated by precipitation then modified by the state and physical
52 features of the catchment. This implies that the integrated information of catchment status might be
53 retrieved by analyzing the discharge time series itself. Focusing on this property, the attempts can be made
54 for capturing the temporal dependence structure of runoff by time series models. The classical time series
55 model, autoregressive integrated moving average (ARIMA), is designed to describe a stationary stochastic
56 process based on the temporal correlation structure of Gaussian random variables (Box and Jenkins, 1976).
57 However, the stationarity of the data is not guaranteed in reality, thus a number of alternative approaches
58 have been suggested. ~~While the application of Fourier analysis is basically for stationary process, the~~
59 ~~analysis using~~ Empirical mode decomposition (Huang et al., 1998) ~~is-overcomes the restriction of~~
60 ~~stationarity a method designed to overcome the drawbacks of Fourier analysis~~ by allowing the frequency
61 and local variance of a time series to vary within a component and to separate the signals adaptively by
62 scale. Autoregressive Conditional Heteroskedasticity (ARCH) models ~~lose~~ the assumption of stationarity
63 to a certain extent so that variance is not constant, however models the variance in a similar way to
64 ARIMA. Although ~~the~~ inventions and efforts to overcome the limitation of stationarity ~~have been~~ made,
65 it seems still inadequate to model dynamic changes of hydrological processes with these time series
66 models.

67 Alternatively there is a statistical concept, ~~the~~ copulas, which has advantages to model the multivariate
68 dependence independently from marginals and recently adopted in the field of hydrology. A Copula (Sklar,
69 1959) is a multivariate probability distribution designed to flexibly model dependence structure in the
70 uniform (quantile) domain. The use of copulas in hydrology can be found for the assessment of extreme
71 events by considering flooding as a joint behavior of peak and volume (De Michele and Salvadori, 2003).
72 Copulas have been applied to describe the spatio-temporal uncertainty of precipitation (Bárdossy and

Pegram, 2009) or the inhomogeneity of groundwater parameters (Bárdossy and Li, 2008). Asymmetry of dependence in a time series can be tested in the framework of a finite state Markov chain's transition probability matrix (Sharifdoost et al., 2009). Dissimilarity measures can be defined by means of a copula modelling the correlation structure of pairs of discharge time series in order to identify the similarity of catchments with the purpose of transferring catchment properties from one to the other (Samaniego et al., 2010). We aim at utilizing copulas as an alternative to classical time series models and an efficient tool for time series analysis to overcome these hydrological challenges.

The main interest of this study is to ~~precisely~~ assess the human intervention and climate change impacts on hydrological regime for the strategy of future development in the region. For achieving this goal, 7 daily discharge gauging stations in South-West Germany (Figure 1), which have 100 years daily discharge records, were chosen and extensively analyzed. The gauging stations Andernach, Kaub, Worms and Maxau are located in the main stream of the Rhine, while Kalkofen, Cochem and Plochingen are located on tributaries. For further analysis, daily precipitation and temperature records in the Baden-Württemberg state of Germany for the last 50 years were obtained from the German Weather Service. Also, 77 discharge records obtained from the Global Runoff Data Centre in Germany were utilized.

~~The following are the novel~~~~What follows is the new~~ aspects introduced in this study: (1) The catchment characteristics ~~s are~~ defined based on copulas and estimated from discharge data. Also the changes of catchment characteristics ~~s~~ are investigated by tracing the temporal change of the ~~these~~ statistics. (2) A method to model systematic changes of dependence structure with the help of copulas is suggested, then its variability and interrelationship ~~with~~ the time series are examined. (3) Anthropogenic impacts are assessed by the discharge - precipitation relation using API and ~~a~~ hydrological model with copula based measures.

This article is divided into five sections. After the introduction, the basic methodology for applying copulas to discharge time series is introduced in the second section. Thirdly, the measures of asymmetry in copulas are defined and estimated for the discharges of the river Rhine and other catchments. The

98 determination of the temporal change of the asymmetry of the copulas is treated in the third section as well.
 99 In the fourth section two topics are treated: (i) the analysis based on copula distances for the observed
 100 discharges and (ii) the comparison of observed discharge with API (Antecedent Precipitation Index) time
 101 series and simulated discharge time series with a hydrological model. The conclusion is given in the fifth
 102 section.

103 2. Methodology

104 In this section, the application of copulas to time series is articulated after a brief introduction of copulas.
 105 The very basics about copulas are presented here and further information can be obtained from (Joe, 1997)
 106 or (Nelsen, 2006).

107 2.1 Basic Methodology

108 In probability theory and statistics, a copula is a multivariate probability distribution for which the
 109 marginal probability distribution of each variable is uniform.

$$110 \quad C : [0,1]^n \rightarrow [0,1] \quad (1)$$

$$111 \quad C(\mathbf{u}^{(i)}) = u_i \quad \text{if } u^{(i)} = (1, \dots, 1, u_i, 1, \dots, 1) \quad (2)$$

112 Any multivariate distribution can be described by a copula and its marginal distributions as was proven by
 113 Sklar's theorem (Sklar, 1959):

$$114 \quad F(\mathbf{x}) = C(F_{x_1}(x_1), \dots, F_{x_n}(x_n)) \quad (3)$$

115 where $F_{x_i}(x_i)$ represents the i-th marginal distribution of a multivariate random variable \mathbf{X} . The copula
 116 density can be derived by taking partial derivatives of the copula:

$$117 \quad c(u_1, \dots, u_n) = \frac{\partial^n C(u_1, \dots, u_n)}{\partial u_1 \dots \partial u_n} \quad (4)$$

118 The advantage of using copulas is that the marginal is detached from the multivariate distribution and
 119 the dependence structure can be examined in the uniform compact domain for different types of data.

120 2.2 Basic Hypothesis of Temporal Copulas

121 For the application of copulas to time series analysis, a stochastic system should be presumed to be
 122 similar to the case of spatial copulas (Bárdossy and Li, 2008): the random variable at time t is described as
 123 $Z(t)$ and in general there may exist non-Gaussian dependency among the elements of $Z(t)$. Then
 124 stationarity is defined for each subset of times $t_1, \dots, t_n \subset N$ and time lag k such that
 125 $\{t_1 + k, \dots, t_n + k\} \subset N$ and for each set of possible values z_1, \dots, z_n :

$$126 \quad \begin{aligned} P(Z(t_1) < z_1, \dots, Z(t_n) < z_n) = \\ P(Z(t_1 + k) < z_1, \dots, Z(t_n + k) < z_n) \end{aligned} \quad (5)$$

127 For the given random function $Z(t)$, a set $S(k)$ containing pairs of ranked values is defined as a
 128 function of time lag k as follows:

$$129 \quad S(k) = \{(F_z(z(t))), (F_z(z(t+k)))\} \quad (6)$$

130 Thus, a 2-dimentional autocopula for stochastic time series is a function of time lag k for the set $S(k)$

131 similar to the case of spatial copula (Bárdossy and Li, 2008):

$$132 \quad C_i(k, u_1, u_2) = P[F_z(Z(t)) < u_1, F_z(Z(t+k)) < u_2] \quad (7)$$

134 where $(u_1, u_2) \in S(k)$. Thus, a 2-dimentional empirical copula density can be constructed based on
 135 conditional empirical frequencies on a regular $g \times g$ grid and kernel density smoothing (Bárdossy, 2006):

$$136 \quad \begin{aligned} c^*\left(\frac{2i-1}{2g}, \frac{2j-1}{2g}\right) = \frac{g^2}{|S(k)|} \\ \cdot \left| \left\{ (u_1, u_2) \in S(k); \frac{i-1}{g} < u_1 < \frac{i}{g} \text{ and } \frac{j-1}{g} < u_2 < \frac{j}{g} \right\} \right| \end{aligned} \quad (8)$$

137 where $|S(k)|$ denotes the cardinality (the number of elements in a set) of set $S(k)$.

138 3. Copula Asymmetry in Discharge Time Series

High and low values might have different dependences in general. Measuring the asymmetry of copulas could reveal substantial aspects of time series data, which are not illuminated in the Gaussian approach. Statistics defined on copula shape and calculated from observed discharge time series we believe to be a new idea. Asymmetry functions are defined on 2-dimensional copulas as a function of time lag k (Li, 2010):

Asymmetry 1 ~~and Asymmetry2 are is~~ defined as:

$$A_1(k) = E[(U_t - 0.5)(U_{t+k} - 0.5)((U_t - 0.5) + (U_{t+k} - 0.5))] \\ = \int_0^1 \int_0^1 (u_t - 0.5)(u_{t+k} - 0.5)(u_t + u_{t+k} - 1) c(u_t, u_{t+k}) du_t du_{t+k} \quad (9)$$

$$A_2(k) = E[-(U_t - 0.5)(U_{t+k} - 0.5)((U_t - 0.5) - (U_{t+k} - 0.5))] \\ = \int_0^1 \int_0^1 -(u_t - 0.5)(u_{t+k} - 0.5)(u_t - u_{t+k}) c(u_t, u_{t+k}) du_t du_{t+k} \quad (10)$$

~~$$A_1(k) = E[(U_t - 0.5)(U_{t+k} - 0.5)((U_t - 0.5) + (U_{t+k} - 0.5))] \quad (9)$$~~

Asymmetry 2 is defined as:

~~$$A_2(k) = E[-(U_t - 0.5)(U_{t+k} - 0.5)((U_t - 0.5) - (U_{t+k} - 0.5))] \quad (10)$$~~

where $u_t = F_Z(z(t))$, $u_{t+k} = F_Z(z(t+k))$. Figure 2 shows an idealization of the ~~two~~ asymmetries between a pair of variables $U(t)$ and $U(t+k)$, showing that the tails of the distributions have a large impact on each type of asymmetry. The measure of asymmetry ~~(i)~~ compares the dependency between low and high values and ~~(ii)~~ quantifies how much it is not symmetric. For example, in a 2-dimensional copula, $A_1(k)$ is positive if the probability density is higher in the upper right corner than in the lower left corner. On ~~the contrary the other hand~~, $A_1(k)$ is negative if the probability density is higher in the lower left corner ~~than in the upper right~~. $A_2(k)$ is the asymmetry for the other diagonal of a 2-dimensional copula. Figure 3 shows the scatterplot of ranked values of a discharge time series with time lag $k = 1$ as a sample of an empirical autocopula and its relation with storm hydrographs. This figure displays (i) where each pair of values on a hydrograph can be plotted on an empirical copula, demonstrating that (ii) the dependence structure is not symmetric especially for $A_2(k)$.

164 ~~This illustration provides the insight that asymmetry can be related to the shape of a unit hydrograph as~~
 165 ~~well as the notion that asymmetry might be used for advanced modeling of hydrological time series.~~
 166 ~~Figure 3 shows the scatterplot of ranked values of a discharge time series with time lag $k = 1$ as a sample~~
 167 ~~of an empirical autocopula, demonstrating the structure is not symmetric especially for $A_2(k)$.~~

168 3.1 Asymmetry and catchment characteristics

169 Asymmetries can be considered as statistics calculated from the observed discharge time series and ~~leads~~
 170 ~~to have~~ an important assumption can be made: ‘assymetry2 is related to catchment characteristics’. This
 171 idea will be ~~intensively~~ discussed ~~u~~and demonstrated in this section. Figure 5 (upper left) shows parts of
 172 the hydrographs of 7 gauging stations in southwest Germany.

173 First, an important ~~and obvious~~ natural property of discharge seen in this figure is that the durations of
 174 high flow and low flow periods ~~areis~~ not symmetric: Flood events, which are initiated by rainfall or
 175 snowmelt, do not continue for a long time because the duration of runoff to rivers is comparatively short.
 176 On the other hand, discharge keeps decreasing and stays low for no rain periods. This means that, if two
 177 consecutive values in a time series are chosen for small time lag k , these two values are likely to be less

178 correlated for high values but more correlated for low values, which leads to negative value of $A_1(k)$.

179 This implies that the intrinsic temporal distribution of precipitation can be investigated based on this
 180 asymmetry, possibly with advanced asymmetry functions such as bivariate moments based on L-moments
 181 (Brahimi et al., 2015).

182 ~~This asymmetry can be related to the intrinsic temporal distribution of precipitation.~~

183 Second, the rates of increase and decrease of discharge ~~areis~~ not symmetrical: Soon after the rainfall, the
 184 river flow rises sharply. Once the rain stops and peak discharge is observed, then the water level starts to
 185 decrease, typically more slowly on the recession than the rising limb of the hydrograph, which leads to
 186 negative values of $A_2(k)$ for small time lags k . This asymmetry can be related to the shape of the

- Formatted: Not Raised by / Lowered by
- Formatted: Font: (Default) Times New Roman, 12 pt
- Formatted: Font: (Default) Times New Roman, 12 pt
- Formatted: Text, Left
- Formatted: Font: (Default) Times New Roman, 12 pt

hydrograph, and therefore the characteristics of the runoff and catchment. In addition, it can be said the annual cycle in Figure 4 is not symmetric in the same sense a unit hydrograph is not symmetric.

The change of $A_2(k)$ with time lag k [days] is now discussed. The point is that these statistics for small time lags k can be more related to the catchment and rainfall characteristics of the region, while asymmetry for larger time lags k can capture the inter-seasonal characteristic of the climate in the region.

In order to reduce such seasonal impacts on the analysis of hydrological time series, deseasonalization measures can be applied, for example, for daily stream flow (Grimaldi, 2004). Adopting this method, all the time series are normalized in this study.

~~In order to reduce this seasonal impact, normalization was adopted for the time series similar to z score in the following way. First, the annual cycle of the mean μ_i on the i -th calendar day is calculated as the expectation of the random variable X_i on the i -th calendar day. Then, the annual cycle of the mean μ_i^* is calculated as a smoothed version of μ_i by linearly weighting the neighboring values along i and summing them up. The smoothed annual cycle of standard deviations σ_i^* (Figure 4 left) can be obtained in the same way. Then the normalized time series is defined by dividing the original time series $Z(t)$ by σ_i^* after subtracting μ_i^* as follows~~

$$Z_{norm}(t) = \frac{Z(t) - \mu_t^*}{\sigma_t^*} \quad (11)$$

~~and smoothed by linear weighting~~

$$\begin{aligned} \mu_{t|365} &= E[X_{t|365}] \\ \mu_{t|365}^* &= \frac{1}{2N} \sum_{i=0}^{N/2} \left(\frac{1}{2} - \frac{i}{N} \right) (\mu_{t+i|365} + \mu_{t-i|365}) \end{aligned} \quad (11)$$

where $t|365$ is $t \pmod{365}$ and represents calendar day at time t [day]. ~~X_i denotes the random variable of discharge, μ_i denotes mean and μ_i^* denotes mean after smoothing on calendar day i respectively. After~~

Formatted: Lowered by 15 pt

Field Code Changed

Formatted: Text

subtraction of the annual mean from the original time series $Z(t)$, the annual cycle of standard deviation is defined.

$$\sigma_{t|365} = E \left[\sqrt{(X_{t|365} - \mu_{t|365})^2} \right] \quad (12)$$

$$\sigma_{t|365}^* = \frac{1}{2N} \sum_{i=0}^{N/2} \left(\frac{1}{2} - \frac{i}{N} \right) (\sigma_{t+i|365} + \sigma_{t-i|365})$$

Figure 4 shows the annual cycles after smoothing described by equations (11) and (12). By subtracting the annual mean cycle and dividing by annual standard deviation cycle, the normalized time series is defined.

$$Z_{norm}(t) = \frac{Z(t) - \mu_{t|365}^*}{\sqrt{\sigma_{t|365}^*}} \quad (13)$$

Figure 5 (upper right) shows parts of normalized discharge time series from the 7 gauging stations. It should be noted that the process still appears to be non-Gaussian after this transformation and the seasonality for small time lags k might not have been fully eliminated. Figure 5 (bottom left and bottom right) shows the variation of asymmetry functions for 7 discharge time series corresponding to time lag k , similar to ~~the~~ correlograms, in addition to the confidence interval of Gaussian process.

The confidence intervals in the figures are gained by calculating $A_2(k)$ for 100 realizations of stationary Gaussian process which are fitted to the observed discharge of Andernach. The result shows that the process is clearly different from Gaussian and the influence of asymmetry is significantly large.

It can be seen that the variation of $A_2(k)$ of discharge without normalization (Figure 5 bottom left) has a larger impact of seasonality for bigger k ($k > 40$), while its impacts are mitigated after the normalization (Figure 5 bottom right). Furthermore, as a consequence of normalization, a sharp drop down of $A_2(k)$ for small time lags k emerged which might be regarded as a catchment indicator. Therefore, the selected/critical properties for small time lags k is formulated by (i) taking the minimum value of $A_2(k)$ for the time lag $k < 50$ and (ii) the lag k at the minimum of asymmetry2:

$$A_{2,\min} = \min_{k < 50} A_2(k) \quad (12)$$

$$L_{2,\min} = \min_{0 < k < 50} \{k; A_2(k) = A_{2,\min}\} \quad (13)$$

The question is whether they are really related to catchment characteristics. Now, these statistics estimated for 77 discharge data recorded at the gauging stations in Germany are compared with the catchment area as one of the simplest possible indicators of the catchment as shown in Figure 6: $A_{2,\min}$ - area (Figure 6 top) and shows a more clear linear relation than $L_{2,\min}$ - area (Figure 6 middle) are both showing a linear relationship with the log-scaled x-axis of catchment area, with positive correlation. There seems also to be a the linear relation between while the dispersions $A_{2,\min}$ and $L_{2,\min}$ - as a consequences of the above relationships in, for the smaller catchments are big for both cases. The correlation between $A_{2,\min}$ and $L_{2,\min}$ (Figure 6 bottom) is slightly positive.

This demonstrates that the information extracted from discharge is related to the basic information of its catchment to a certain extent. Since the principal objective is to assess anthropogenic impacts, the idea introduced now is to use this measure for evaluating the catchment change by calculating chronological changes of $A_{2,\min}$.

3.2 Time Series Analysis with Asymmetry

Temporal change of asymmetry $A_2(k, t)$ is defined on the set representing a moving time window of size w .

$$S^*(k, t) = \left\{ (F_Z(z(a))), (F_Z(z(a+k))); t - \frac{w}{2} < a < t + \frac{w}{2} \right\} \quad (14)$$

$$\begin{aligned} A_2(k, t) &= E[-(U_t - 0.5)(U_{t+k} - 0.5)((U_t - 0.5) - (U_{t+k} - 0.5))] \\ &= \int_0^1 \int_0^1 -(u_t - 0.5)(u_{t+k} - 0.5)(u_t - u_{t+k})c(u_t, u_{t+k})du_t du_{t+k} \end{aligned}$$

(15)

247 where $u_t \in U_t, u_{t+k} \in U_{t+k}, (u_t, u_{t+k}) \in S^*(k, t)$. Then the minimum of asymmetry2 and lag k at the
 248 minimum of asymmetry2 at time t are given by

$$249 \quad A_{2,\min}(t) = \min_{k < 30} A_2(k, t) \quad (16)$$

$$250 \quad L_{2,\min}(t) = \min_{0 < k < 30} \{k; A_2(k, t) = A_{2,\min}(t)\} \quad (17)$$

251 Figure 7 shows the temporal changes of $A_{2,\min}(t)$ with window size $w = 3000$ [days] for 7 gauging
 252 stations in southwest Germany in addition to the confidence interval calculated for 100 times
 253 independently generated Gaussian process.

254 The comparison of $A_{2,\min}(t)$ from observed discharges with $A_{2,\min}(t)$ from a Gaussian process exhibits
 255 (i) the influence of asymmetry in discharge is significantly large as ~~it~~ was seen in Figure 5; (ii) The
 256 fluctuations of $A_{2,\min}(t)$ of 7 observed discharge time series appear to be bigger than the one calculated for
 257 a realization of a Gaussian process ~~and~~; (iii) $A_{2,\min}(t)$ of these 7 discharge records shows a similar trend:
 258 there are big drop-downs around 1945 and after 1980 for all the discharges.

259 However, it cannot be ascertained whether this is caused by the simultaneous change of the catchments,
 260 the long term meteorological behavior in the region or just randomness in the stationary process. To
 261 overcome this, temporal behavior of discharge and temperature were first checked by calculating the mean,
 262 the standard deviation and the minimum ~~in a time window centered on~~ time t defined by

$$\begin{aligned} 263 \quad Mean(t) &= \frac{1}{w} \int_{t-w/2}^{t+w/2} z(a) da \\ Std(t) &= \sqrt{Var(t)} = \frac{1}{w} \left(\int_{t-w/2}^{t+w/2} (z(a) - E[Z(t)])^2 da \right)^{\frac{1}{2}} \\ Min(t) &= \min \left\{ Z(a); t - \frac{w}{2} < a < t + \frac{w}{2} \right\} \end{aligned} \quad (18)$$

264 where w is the size of time window. Figure 8 shows ~~the~~ moving average and moving standard deviation of
 265 discharge records with windows size $w = 3000$ [days], but it is hard to say whether the behavior around
 266 1945 and after 1980 is unusual. Figure 9 shows mean and minimum of temperature in the time window

267 | ~~of~~with size 365 [days] which correspond to annual mean and minimum. Roughly speaking, there are
268 certain cold periods around 1940, 1955 and 1985, which might influence the snow accumulation and
269 melting in the region, but the relation with asymmetry2 is rather obscure.

270 What seems to be a useful outcome from the above exploratory analysis is that (i) the behavior of
271 asymmetry2 is different from catchment to catchment showing a statistical relation with the catchment area
272 and (ii) temporal behaviors of asymmetry2 of 7 discharges time series are dependent on each other, which
273 implies the existence of a background mechanism common to the region.

274 4. Analysis of hydrological time series with Copula Distance

275 As an alternative to copula asymmetry, which emphasizes the behavior ~~in~~the corner~~s~~s of copulas,
276 copula distance is here suggested so that the characteristic behavior can be captured in the entire domain of
277 the copula. Calculating this for each time step for different time series and comparing them hopefully
278 exhibits the changes of dependence structure and therefore the catchment change.

279 4.1 Introduction of Copula Distance

280 The basic idea behind the copula distance is to apply the Cramér-von Mises type distance

281
$$D = \int_0^1 \int_0^1 \left(C^*(u_1, u_2) - C(u_1, u_2) \right)^2 du_1 du_2 \quad (19)$$

Field Code Changed

282 | ~~which~~by design measures the goodness of fit between two distribution functions~~to~~ to two copulas. This
283 type of distance was tested to measure the difference between empirical and theoretical copula~~s~~s in the
284 bootstrap framework for the evaluation of spatial dependence of ground water quality (Bárdossy, 2006).
285 For the analysis of time series data, it still needs to be carefully thought out how (and which) copulas
286 should be chosen.

287 4.1.1 Introduction of Copula Distance to single time series

288 In order to apply the concept of copula distance to time series, the adoption of two copulas in different
289 time scales is considered. An empirical copula can be obtained from an entire time series which contains

the averaged information of all the time points (*global copula*). Another empirical copula can be obtained for a certain time window of width w centered at time step t (*local copula*). In order to make the concept clear, two sets containing pairs of ranked values with different time scales are specified.

$$S_{global}(k) = \left\{ \left(F_Z(z(t)), F_Z(z(t+k)) \right); t_1 < t < t_n \right\} \quad (20)$$

$$S_{local}(k, t) = \left\{ \left(F_Z(z(a)), F_Z(z(a+k)) \right); t - \frac{w}{2} < a < t + \frac{w}{2} \right\} \quad (21)$$

$S_{local}(k, t)$ can be interpreted as a moving time window where the reference time t is set to the middle of the window of size w , while $S_{global}(k)$ represents a set of the entire time series. *Global copula* and *local copula* are the empirical autocopula densities defined on these sets based on Equation ~~(8)~~~~(8)~~~~(8)~~, there denoted by $c_{global}^*(\mathbf{u})$ and $c_{local}^*(\mathbf{u}, t, w)$ respectively for the n -dimensional case. In this analysis, 3000 [days] for the time window w and a 3-dimensional copula separated with 1 day gap between each variable are employed. This means that

$$\mathbf{u} = (u_0, u_1, u_2) \quad (22)$$

where $u_0 = F_z(Z(t))$, $u_1 = F_z(Z(t+1))$, $u_2 = F_z(Z(t+2))$, then the deviation of local copula from global copula is defined by

$$\Delta c(\mathbf{u}, t) = c_{local}^*(\mathbf{u}, t) - c_{global}^*(\mathbf{u}) \quad (23)$$

For the first approach, the comparison of dependence structures between entire and local time series is done for detecting unusual dependence structures. To this end, *copula distance type1* is defined by taking the copula distance between global and local copula~~s~~ at each time step t

$$\begin{aligned} D_1(c, t) &= \int_0^1 \dots \int_0^1 \left(c_{global}^*(\mathbf{u}) - c_{local}^*(\mathbf{u}, t) \right)^2 du_1 \dots du_n \\ &= \int_0^1 \dots \int_0^1 \Delta c(\mathbf{u}, t)^2 du_1 \dots du_n \end{aligned} \quad (24)$$

Second, *copula distance type 2* is introduced for indicating the point at which the structure of copulas starts to change. For this method, the distance between two local copulas is calculated ~~at two instants; from the 2~~ ~~time intervals~~

$$D_2(c, t) = \int_0^1 \dots \int_0^1 \left(c_{local}^* \left(\mathbf{u}, t - \frac{w}{2} \right) - c_{local}^* \left(\mathbf{u}, t + \frac{w}{2} \right) \right)^2 du_1 \dots du_n \quad (25)$$

Note that reference time is set to the middle of both time windows and shifted for $w/2$ [days] from each other where the size of the time windows is w . Therefore, there is no overlapping part between the two time intervals of these two local copulas. For the comparison, the moving variance is introduced as follows:

$$\begin{aligned} E[Z(t)] &= \frac{1}{w} \int_{t-w/2}^{t+w/2} z(a) da \\ Var(t) &= \frac{1}{w} \int_{t-w/2}^{t+w/2} \left(z(a) - E[Z(t)] \right)^2 da \end{aligned} \quad (26)$$

Figure 10 shows the result of $D_1(t)$, $D_2(t)$ and $Var(t)$ in the moving time window for the normalized discharge time series between 1940 to 2000 at 4 gauging stations located in the main stream of the Rhine (Andernach, Maxau) and its two different tributaries (Cochem, Plochingen) in addition to the 90 % confidence intervals calculated for the Gaussian process fitted to the discharge data of Andernach.

First of all, the values of ~~these 2~~ $D_1(t)$ ~~and~~ $D_2(t)$ ~~measures~~ at Cochem and Plochingen are bigger and more fluctuating ~~than~~ in general. The reason could be that their catchments and discharges are smaller, thus more sensitive to changes. Second, it can be said that the dependence structure is not homogeneous over the time period, but the local copula clearly deviates from the global copula for certain time periods. For example, the value of $D_1(t)$ is remarkably big around 1947, 1982 and 2000 for all the 4 discharge records (~~indicated~~~~pointed~~ by white arrows). $D_2(t)$ is also big around 1977 for all the data. ~~Theis~~ signal of $D_2(t)$ implies that a simultaneous change of runoff behavior occurred in this region ~~inat~~ 1977, which can be related to the high value of $D_1(t)$ at 1982. $Var(t)$ is also changing, but ~~athe~~ direct relation with $D_1(t)$

330 and $D_2(t)$ is hard to recognize. Also the confidence interval of the Gaussian process is clearly smaller
 331 than the observed one. This indicates the copula distances of the stationary process are small while the
 332 nature process is non-stationary and its dependence structure is more varying.

333 For copula distance type1, the global copula can be considered as an average state of the copula, while
 334 the local copula can be regarded as a realization of a possible state of a copula at time step t . This concept
 335 can be comparable to variance and leads to a new measure, *copula variance*, which is the summation of
 336 copula distances between global and local copula over the time.

$$337 \quad Var_{cop}(c) = \frac{1}{t_n - t_1} \int_{t_1}^{t_n} D_1(c, t) dt \quad (27)$$

338 ~~Table 1~~ ~~Table 1~~ ~~Table 1~~ shows the variance and copula variance calculated for the 4 discharge data. The
 339 result demonstrates that copula variance of the time series can be higher, even if the conventional variance
 340 is lower for example in case of Maxau.

341 4.1.2 Copula Distance for two time series

342 In the previous section, copula variance was defined as a measure of the variability characteristic of the
 343 copula itself. Here, it is ~~determined~~ ~~examined~~ whether covariance can be defined for two copula densities c_1
 344 and c_2 from two time series as *copula distance type3*, which shows whether the variability characteristic of
 345 copulas is related to each other. The measure introduced is :

$$346 \quad D_3(c_1, c_2, t) = \int_0^1 \dots \int_0^1 \Delta c_1(\mathbf{u}, t) \Delta c_2(\mathbf{u}, t) du_1 \dots du_n \quad (28)$$

347 where

$$348 \quad \begin{aligned} \Delta c_1(\mathbf{u}, t) &= c_{1,local}^*(\mathbf{u}, t) - c_{1,global}^*(\mathbf{u}) \\ \Delta c_2(\mathbf{u}, t) &= c_{2,local}^*(\mathbf{u}, t) - c_{2,global}^*(\mathbf{u}) \end{aligned} \quad (29)$$

349 By its definition, the value of $D_3(t)$ can be related to $D_1(t)$ because $D_3(t)$ compares the deviation of local
 350 copulas from global copulas in a similar way to $D_1(t)$ in Equation (26). In order to reduce the influence of

351 $D_1(t)$ on $D_3(t)$, *copula distance type4* is introduced as a normalized measure bounded between -1 and 1
 352 analogous to correlation.

$$353 \quad D_4(c_1, c_2, t) = \frac{D_3(c_1, c_2, t)}{\sqrt{D_1(c_1, t)} \cdot \sqrt{D_1(c_2, t)}} \quad (30)$$

354 where $|D_4(c_1, c_2, t)| \leq 1$. For comparison, covariance and correlation in a moving window are introduced for
 355 two random variables $Z_1(t)$ and $Z_2(t)$ as follows:

$$356 \quad Cov(t) = \int_{t-w/2}^{t+w/2} (z_1(a) - E[Z_1(t)])(z_2(a) - E[Z_2(t)]) da \quad (31)$$

$$357 \quad Corr(t) = \frac{Cov(t)}{\sqrt{Var(Z_1(t))} \cdot \sqrt{Var(Z_2(t))}} \quad (32)$$

358 Figure 11 shows the copula distance between two time series $D_3(t)$ and $D_4(t)$ in addition to the
 359 covariance and correlation in [a](#) moving time window.

360 First, it can be said that the behavior of covariance and correlation in a moving window are different
 361 from $D_3(t)$ and $D_4(t)$. This implies these two copula based statistics exhibit different properties of the
 362 time series from ordinary statistics. Second, $D_3(t)$ shows high values around 1947, 1982 and 2000, which
 363 is ~~similar~~ to the case of $D_1(t)$ in Figure 10. This indicates that unusual states of copulas in 4 discharge
 364 time series can be related to each other. Third, $D_4(t)$ is in general high except for the period around 1970
 365 and 1990. This means, the temporal behavior of dependence structures for these 4 discharges are actually
 366 similar except for these periods even if $D_1(t)$ and $D_3(t)$ are small.

367 Copula covariance and copula correlation can be defined similar to copula variance in order to quantify
 368 the overall behavior of two time series.

$$369 \quad Cov_{cop}(c_1, c_2) = \frac{1}{t_2 - t_1} \int_{t_2}^{t_1} D_3(t) dt \quad (33)$$

$$370 \quad Corr_{cop}(c_1, c_2) = \frac{Cov_{cop}(c_1, c_2)}{\sqrt{Var_{cop}(c_1)} \cdot \sqrt{Var_{cop}(c_2)}} \quad (34)$$

371 where $|Corr_{cop}(c_1, c_2)| \leq 1$ and its derivation can be found in appendix A. In ~~Table 2~~Table 2~~Table 2~~, these
372 copula based statistics are compared with ordinary statistics. For example, Cochem and Plochingen are
373 located remotely in different tributaries, thus covariance and correlation are lower than the others, but
374 copula covariance and copula correlation are not the lowest.

375 The measures using copula distance are different from the conventional statistics. This behavior can be
376 explained by the fact that the autocopula has more substantial information about temporal dependence
377 structure than the autocorrelation. Using these measures might enable us to take advantage of a different
378 way of seeing the dependence between time series.

379 What is new in the analysis of this section is that (i) measures based on copula distance show the
380 different properties of time series in comparison to conventional statistics and (ii) there are significant
381 signals of copula distances for certain time periods in common to all the discharge data.

382 **4.2 Copula based Stochastic Analysis with API and a Hydrological Model**

383 The difficulty of analyzing discharge time series in order to detect catchment change is that it is not clear
384 whether the temporal change of stochastic information is caused by catchment change or merely by
385 random behavior of precipitation. To gain an understanding of this process, we attempted to eliminate the
386 influence of precipitation using, first, an Antecedent Precipitation Index (API) (~~antecedent-precipitation~~
387 ~~index~~) for comparison with discharge , second, using a hydrological model with the parameter sets
388 calibrated and fixed for the entire simulation time period.

389 **4.2.1 Copula Distance Analysis with API**

390 An API (~~Antecedent Precipitation Index~~) time series, which is generated from observed precipitation
391 time series and behaves similarly to discharge, is used instead of precipitation.

392
$$API(t+1) = \alpha API(t) + P(t+1) \quad (35)$$

Field Code Changed

where $P(t)$ is daily precipitation [mm/day], $API(t)$ is time series of API [mm/day] and $\alpha = 0.85$ was chosen. The assumption for this method is that the API time series has the stochastic information purely originated from the precipitation, while observed discharge is ~~supposed to be~~ influenced by both catchments and precipitation's characteristics. If the stochastic information derived from these two data sets is the same, this indicates that the stochastic turbulence is originating from precipitation; otherwise the change is from the catchment.

For this investigation, precipitation data was carefully chosen for 4 regions (northwest, northeast, southwest and central) of Baden-Württemberg (Germany) so that they have several almost continuous daily records between 1935 and 2005. Figure 12 shows the locations of measuring stations. The precipitation time series were aggregated into one for each region by taking their daily average, then 4 API time series ~~were~~ calculated in total by Equation ~~(35)(35)(35)~~. Figure 13 shows the ~~resulting of~~ copula distances $D_1(t), D_2(t)$ and moving average $Var(t)$ for API time series with the 90% confidence intervals of the Gaussian process. Figure 14 shows the result of copula distances $D_3(t), D_4(t)$ and moving covariance and correlation for API time series.

What can be recognized first ~~from in this~~ Figure 13 is that the magnitudes of $D_1(t)$ and $D_2(t)$ are smaller than the case of discharge. This is considered to ~~be happen as~~ a result of aggregation of precipitation time series and adoption of API, but some signals can be still identified: $D_1(t)$ around 1947 and 2000 is high, but not ~~as high much~~ for 1982. The signal of $D_2(t)$ which was detected around 1977 in Figure 11 does not seem to exist for API. This ~~is can be~~ even more clear for $D_3(t)$ in Figure 14 ~~in~~ that there is no common change of the dependence structure around 1982 in API time series. This is interesting due to the following implications: (i) the noises of $D_1(t)$ in ~~Figure 13 Figure 13 Figure 13~~ were reduced and signals in common were amplified (ii) the unusual state of the copula around 1982 is not caused ~~not~~ by precipitation, but could be caused by the catchment change.

416 For further verification, copula distance type3 and type4 between discharge and API time series were
417 calculated as shown in Figure 15. This result also shows there is no clear relation between API and
418 discharge time series around 1982.

419 4.2.2 Copula based analysis with a hydrological model

420 ~~API time series were calculated by spatially aggregating several daily precipitations records in each region~~
421 ~~of Baden-Württemberg state.~~ In this section, simulated discharges time series are generated by a
422 conceptual hydrological model, HBV (Bergström 1976 ; Bergström, Singh, and others 1995) ,which takes
423 daily precipitations and temperatures records as input and simulates discharges for smaller catchments as
424 ~~an example more robust sample~~ of discharge, to compare with observed discharge in order to check if
425 differences might occur due to the method.

426 Thus the idea behind this methodology is similar to the case of API: ~~a~~ hydrological model with the
427 parameters fixed for the entire time period represents the catchment not influenced by anthropogenic
428 impacts. Then, the discharges simulated by this model should not ~~depend~~ ~~reflect~~ ~~on the~~ catchment change,
429 while observed discharge is assumed to be influenced by both catchment and precipitation.

430 For the study area, ~~the~~ Upper Neckar Catchment was chosen as ~~shown~~ ~~drawn~~ in Figure 12. One
431 parameter set needed for this model constitutes of 13 parameters which are calibrated based on the Nash–
432 Sutcliffe model efficiency coefficient using the simulated annealing algorithm for the period between 1960
433 and 2000. Then, 30 parameter sets are independently calibrated in total and, subsequently, 30 simulated
434 discharges time series are generated to compare with one observed discharge.

435 Figure 16 shows the result of copula based analysis calculated for single time series
436 $(D_1(t), D_2(t), A_{2,min}(t))$. It can be seen that $A_{2,min}(t)$ in Figure 16 (top) that (i) fluctuations of $A_{2,min}(t)$
437 of observed and simulated discharge are locally identical. This implies that the short term behavior of
438 $A_{2,min}(t)$ is originated from the temporal behavior of precipitation but (ii) there exists a change of trend
439 around 1976: $A_{2,min}(t)$ of observed discharge is slightly bigger than simulated before 1976, while

440 $A_{2,\min}(t)$ of observed discharge clearly undershoot the simulated ones of after 1976. This change of trend
 441 was also seen in the previous analyses ($D_2(t)$ in Figure 10). Furthermore, $D_1(t)$ in Figure 16 (middle) is
 442 high before 1976 which indicates the state of the copula is different from the rest, while the result of
 443 simulated discharges does not show such tendency. $D_2(t)$ in Figure 16 (bottom) indicates the change of
 444 dependence structure happened around 1970 and 1977. These results using the HBV model indicate the
 445 change of the dependence structure detected using copulas around 1976 is not caused by the random
 446 behavior of precipitation, but by the behavior of the catchment itself.

447 The fact and the notion obtained in this section is that (i) both results from API and HBV based on
 448 copula measures indicate that the catchment changed around 1976 and (ii), by comparing the simulated
 449 discharge with observed discharge, the origin of the change of stochastically information can be assessed.

451 Conclusion

452 In this paper the application of copulas for hydrological time series data is newly explored for the
 453 detection of catchment characteristics and their temporal changes.

454 1. A Copula based measure, asymmetry, was defined and newly applied for the identification of
 455 catchment characteristics. Indeed, it ~~was is presumed~~ presented that asymmetry2 ~~is can be~~ related to the
 456 runoff characteristics.

457 2. The relation between the minimum of asymmetry2 and catchment characteristics was tested for 77
 458 discharge records. Asymmetry2 has a certain relation especially with ~~the size of bigger~~ catchments and this
 459 strengthens the notion that asymmetry2 can be used as a statistic to explain the catchment state.

460 3. Temporal change of asymmetry2 was calculated as an index of the catchment state and demonstrated
 461 it keeps changing coincidentally with time. However, it is difficult to explain the causality, at least, by long
 462 term behavior of discharge and temperature time series.

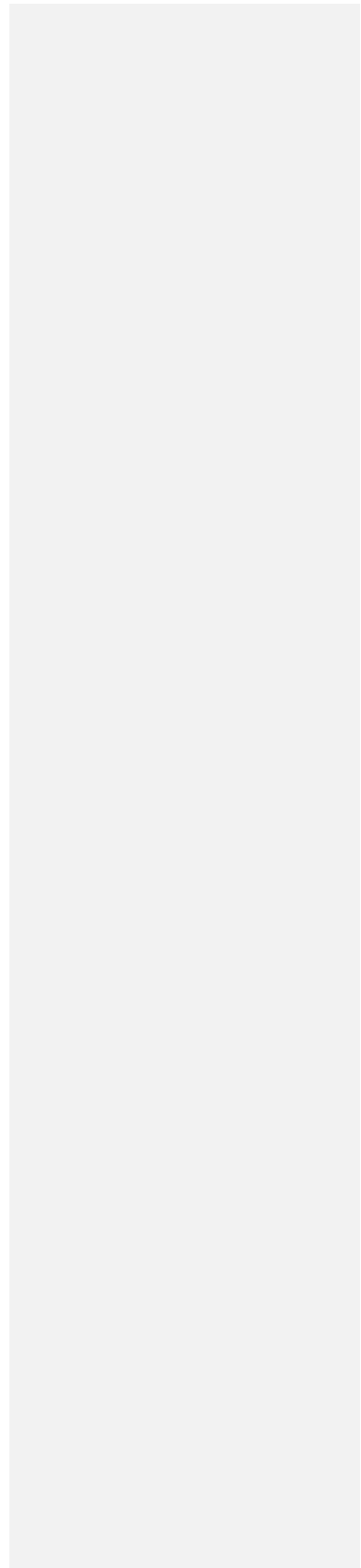
463 4. A method based on copula distance was examined for the investigation of temporal behavior of
464 hydrological time series. This measure can detect the time period where dependence structure is unusual
465 and its interdependency. Clear signals were detected that the dependence structure is unusual for a certain
466 time period and the signal was not found by investigating the time series with variance, covariance or
467 correlation.

468 5. API time series were generated for each region in the Baden-Württemberg state and simulated
469 discharge time series were generated using the HBV model for the Upper Neckar Catchment. These are the
470 data not influenced by ~~the~~ catchment change, thus compared with observed discharge to assess the
471 anthropogenic impacts. The results showed that there was a signal detected only in the observed discharge
472 around 1982, but not in the API or simulated time series, which implies the anthropogenic impacts on the
473 catchment. Also it was shown in the results of copula asymmetry that ~~the difference of $A_{2,min}(t)$ between~~
474 ~~observed and simulated discharge was not constant, but~~ the trend clearly changed around 1976.

475 The results of copula based analysis of hydrological time series seem to support the assumption that the
476 catchment had started to change around 1976 and stayed unusual until 1990. These changes could
477 correspond to the construction of flood retention basins started around 1982 (Lammersen et al., 2002) and
478 ecological flooding strategy, which let small floods to happen for the rehabilitation of ecological systems
479 in the floodplain, introduced in the Upper Rhine since 1989 (Siepe, 2006).

480 Copulas can be seen as an alternative method to analyze ~~the~~ hydrological time series data by focusing on
481 the dependence structure, but further exploratory applications and theoretical developments are expected.
482 The copula based measures introduced in this study can be related to the potential model uncertainty, that
483 is, how much the natural system is varying. Empirical autocopula analysis is a more data driven approach
484 which retains more information than the copulas estimated with parametric methods, but it is also
485 numerically demanding. The effective way to analyze time series and build up a time series model based
486 on copulas can be further explored.

Field Code Changed
Field Code Changed
Field Code Changed



489 **Appendix A**

490 Suppose that a random variable at time t is denoted as $X(t)$ and $c_X(\mathbf{u}, t)$ is an autocopula obtained from
 491 $X(t)$. Assuming $c_{X,mean}(\mathbf{u})$ as an average state of $c_X(\mathbf{u}, t)$, deviation of copula $\Delta c_X(\mathbf{u}, t)$ at time t is
 492 defined by

$$493 \quad \Delta c_X(\mathbf{u}, t) = c_X(\mathbf{u}, t) - c_{X,mean}(\mathbf{u}) \quad (A1)$$

494 For the empirical case, $c_X(\mathbf{u}, t)$ and $c_{X,mean}(\mathbf{u})$ can be regarded as local copula and global copula
 495 respectively similar to Equation ~~(29)~~(29)(29). Since global and local copula are empirical copula density as
 496 defined in equation ~~(8)~~(8)(8), $\Delta c_X(\mathbf{u}, t)$ can be regarded as a vector of values on finite number of grids:

$$497 \quad \Delta \mathbf{c}_X(t) = (\Delta c_{X,1}(t), \Delta c_{X,2}(t), \dots, \Delta c_{X,i}(t), \dots, \Delta c_{X,N}(t)) \quad (A2)$$

498 where $\Delta c_{X,i}(t)$ denotes the value of copula density at i -th grid and N is the number of grids. From
 499 Cauchy-Schwarz inequality

$$500 \quad \|\Delta \mathbf{c}_X(t)\| \|\Delta \mathbf{c}_Y(t)\| \geq \left| \langle \Delta \mathbf{c}_X(t), \Delta \mathbf{c}_Y(t) \rangle \right|^2 \quad (A3)$$

501 where $\|\Delta \mathbf{c}_X(t)\|$ is norm and $\langle \Delta \mathbf{c}_X(t), \Delta \mathbf{c}_Y(t) \rangle$ is inner product of vector $\Delta \mathbf{c}_X(t)$ and $\Delta \mathbf{c}_Y(t)$. Then

$$502 \quad \begin{aligned} \|\Delta \mathbf{c}_X(t)\| &= \sum_{i=1}^N \Delta c_{X,i}(t)^2 \\ &= \int_0^1 \dots \int_0^1 (\Delta c_X(\mathbf{u}, t))^2 du_1 \dots du_n = D_1(c_X, t) \end{aligned} \quad (A4)$$

$$503 \quad \begin{aligned} &\left| \langle \Delta \mathbf{c}_X(t), \Delta \mathbf{c}_Y(t) \rangle \right|^2 \\ &= \langle \Delta \mathbf{c}_X(t), \Delta \mathbf{c}_Y(t) \rangle = \sum_{i=1}^N \Delta c_{X,i}(t) \cdot \Delta c_{Y,i}(t) \\ &= \int_0^1 \dots \int_0^1 \Delta c_X(\mathbf{u}, t) \Delta c_Y(\mathbf{u}, t) du_1 \dots du_n = D_3(c_X, c_Y, t) \end{aligned} \quad (A5)$$

$$504 \quad \frac{\left| \langle \Delta \mathbf{c}_X(t), \Delta \mathbf{c}_Y(t) \rangle \right|^2}{\|\Delta \mathbf{c}_X(t)\| \|\Delta \mathbf{c}_Y(t)\|} = \frac{D_3(c_X, c_Y, t)^2}{D_1(c_X, t) \cdot D_1(c_Y, t)} = D_4(c_X, c_Y, t)^2 \leq 1 \quad (A6)$$

Therefore $|D_4(c_X, c_Y, t)| \leq 1$ in Equation ~~(30)(30)(30)~~. Above inequality is valid for certain time point t and summing up (A6) for all the time steps t leads to

$$\sum_{t=1}^T (\|\Delta \mathbf{c}_X(t)\| \cdot \|\Delta \mathbf{c}_Y(t)\|) \geq \sum_{t=1}^T |\langle \Delta \mathbf{c}_X(t), \Delta \mathbf{c}_Y(t) \rangle| \quad (\text{A7})$$

where T is the number of time steps. $\|\Delta \mathbf{c}_X(t)\|$ is a norm and can be denoted for simplicity as

$x_t = \|\Delta \mathbf{c}_X(t)\|$. Then

$$\sum_{t=1}^T (\|\Delta \mathbf{c}_X(t)\| \|\Delta \mathbf{c}_Y(t)\|) = \langle \mathbf{x}, \mathbf{y} \rangle \quad (\text{A8})$$

where $\mathbf{x} = (x_1, x_2, \dots, x_T)$, $\mathbf{y} = (y_1, y_2, \dots, y_T)$ for $t = 1 \dots T$. Again from Cauchy-Schwarz inequality

$$|\langle \mathbf{x}, \mathbf{y} \rangle|^2 \leq \|\mathbf{x}\| \|\mathbf{y}\| \quad (\text{A9})$$

where

$$\begin{aligned} \|\mathbf{x}\| \cdot \|\mathbf{y}\| &= \sum_{t=1}^T x_t^2 \cdot \sum_{t=1}^T y_t^2 = \sum_{t=1}^T \|\Delta \mathbf{c}_X(t)\|^2 \cdot \sum_{t=1}^T \|\Delta \mathbf{c}_Y(t)\|^2 \\ &= \sum_{t=1}^T D_1(c_X, t)^2 \cdot \sum_{t=1}^T D_1(c_Y, t)^2 = T^2 \cdot \text{Var}_{cop}(c_X) \cdot \text{Var}_{cop}(c_Y) \end{aligned} \quad (\text{A10})$$

$$\begin{aligned} \langle \mathbf{x}, \mathbf{y} \rangle &= \sum_{t=1}^T (x_t \cdot y_t) = \sum_{t=1}^T (\|\Delta \mathbf{c}_X(t)\| \cdot \|\Delta \mathbf{c}_Y(t)\|) \geq \sum_{t=1}^T |\langle \Delta \mathbf{c}_X(t), \Delta \mathbf{c}_Y(t) \rangle| \\ &= \sum_{t=1}^T D_{3,XY}(t) = T \cdot \text{Cov}_{cop}(c_X, c_Y) \end{aligned} \quad (\text{A11})$$

Then $|\langle \mathbf{x}, \mathbf{y} \rangle|^2 \leq \|\mathbf{x}\| \|\mathbf{y}\|$ indicates

$$\begin{aligned} |\text{Cov}_{cop}(c_X, c_Y)|^2 &\leq \text{Var}_{cop}(c_X) \text{Var}_{cop}(c_Y) \\ |\text{Cor}_{cop}| &= \frac{\text{Cov}_{cop}(c_X, c_Y)}{\sqrt{\text{Var}_{cop}(c_X)} \cdot \sqrt{\text{Var}_{cop}(c_Y)}} \leq 1 \end{aligned} \quad (\text{A12})$$

520 **Acknowledgment**

521 Fundamental research of this paper was initiated by the BfG (German Federal Institute of Hydrology)
522 with financial support. Special thanks are given to the Global Runoff Data Centre (GRDC) in Germany
523 for offering the discharge data and the German Meteorological Service (DWD) for precipitation and
524 temperature data. ~~(The authors thank the reviewers for their care in examining this work. All the authors~~
525 ~~deeply appreciate all the reviewers for the efforts for examining and inspecting this work).~~

Formatted: No underline

526 **References**

527 Bárdossy, a., Pegram, G., 2009. Copula based multisite model for daily precipitation simulation. Hydrol.
528 Earth Syst. Sci. Discuss. 6, 4485–4534. doi:10.5194/hessd-6-4485-2009

529 Bárdossy, A., 2006. Copula-based geostatistical models for groundwater quality parameters. Water Resour.
530 Res. 42, W11416. doi:10.1029/2005WR004754

531 Bárdossy, A., Li, J., 2008. Geostatistical interpolation using copulas. Water Resour. Res. 44, W07412.
532 doi:10.1029/2007WR006115

533 Bergström, S., 1976. Development and application of a conceptual runoff model for Scandinavian
534 catchments, Bulletin Series A, A]: [Bulletin series. Department of Water Resources Engineering, Lund
535 Institute of Technology, University of Lund.

536 Bergstrom, S., 1995. The HBV Model. Singh, V.P. (Ed.), Comput. Model. Watershed Hydrol. 443–476.

537 Box, G.E.P., Jenkins, G.M., 1976. Time series analysis: forecasting and control, revised ed. Holden-Day,
538 San Francisco,USA.

539 Brahimi, B., Chebana, F., Necir, A., 2014. Copula representation of bivariate L-moments: a new
540 estimation method for multiparameter two-dimensional copula models. Statistics (Ber). 1–25.

541 De Michele, C., Salvadori, G., 2003. A Generalized Pareto intensity-duration model of storm rainfall
542 exploiting 2-Copulas. J. Geophys. Res. Atmos. 108, 4067. doi:10.1029/2002JD002534

543 Gao, P., Geissen, V., Ritsema, C., Mu, X.-M., Wang, F., 2012. Impact of climate change and
544 anthropogenic activities on stream flow and sediment discharge in the Wei River basin, China. Hydrol.
545 Earth Syst. Sci. Discuss. 9, 3933–3959. doi:10.5194/hessd-9-3933-2012

546 Grimaldi, S., 2004. Linear parametric models applied to daily hydrological series. J. Hydrol. Eng. 9, 383–
547 391. doi:10.1061/(ASCE)1084-0699(2004)9:5(383)

Formatted: English (U.S.)

548 Huang, N.E., Shen, Z., Long, S.R., Wu, M.C., Shih, H.H., Zheng, Q., Yen, N.-C., Tung, C.C., Liu, H.H.,
549 1998. The empirical mode decomposition and the Hilbert spectrum for nonlinear and non-stationary time
550 series analysis. *Proc. R. Soc. London. Ser. A Math. Phys. Eng. Sci.* 454, 903–995.

551 Joe, H., 1997. *Multivariate models and multivariate dependence concepts*. Chapman&Hall, London.

552 Karlsson, I.B., Sonnenborg, T.O., Jensen, K.H., Refsgaard, J.C., 2014. Historical trends in precipitation
553 and stream discharge at the Skjern River catchment, Denmark. *Hydrol. Earth Syst. Sci.* 18, 595–610.
554 doi:10.5194/hess-18-595-2014

555 Lammersen, R., Engel, H., Van de Langemheen, W., Buiteveld, H., 2002. Impact of river training and
556 retention measures on flood peaks along the Rhine. *J. Hydrol.* 267, 115–124. doi:10.1016/S0022-
557 1694(02)00144-0

558 Li, J., 2010. *Application of copulas as a new geostatistical tool*. PhD Thesis. Nr. 187. University of
559 Stuttgart, Germany

560 Nelsen, R.B., 2006. *An Introduction to Copulas*. Springer, New York. doi:10.1007/0-387-28678-0

561 Pettitt, A.N., 1979. A non-parametric approach to the change-point problem. *Appl. Stat.* 126–135.

562 Samaniego, L., Bárdossy, A., Kumar, R., 2010. Streamflow prediction in ungauged catchments using
563 copula-based dissimilarity measures. *Water Resour. Res.* 46, W02506. doi:10.1029/2008WR007695

564 [Serfling, R., Xiao, P., 2007. A contribution to multivariate L-moments: L-comoment matrices. *J. Multivar.*
565 *Anal.* 98, 1765–1781. doi:10.1016/j.jmva.2007.01.008](#)

566 Sharifdoost, M., Mahmoodi, S., Pasha, E., 2009. A statistical test for time reversibility of stationary finite
567 state Markov chains. *Appl. Math. Sci.* 52, 2563–2574.

568 Siepe, A., 2006. *Dynamische Überflutungen am Oberrhein : Entwicklungs-Motor für die Auwald-Fauna*.
569 Stand 149–158.

570 Singh, S.K., McMillan, H., Bárdossy, A., 2013. Use of the data depth function to differentiate between
571 case of interpolation and extrapolation in hydrological model prediction. *J. Hydrol.* 477, 213–228.
572 doi:10.1016/j.jhydrol.2012.11.034

573 Sklar, A., 1959. *Fonctions de répartition à n dimensions et leurs marges*, Publications de l’Institut de
574 statistique de l’Université de Paris. Publications de l’Institut de Statistique de L’Université de Paris 8.

575 Sugimoto, T., 2014. *Copula based stochastic analysis of discharge time series*. PhD Thesis. Nr. 232.
576 University of Stuttgart, Germany

577 Wu, C.S., Yang, S.L., Lei, Y.P., 2012. Quantifying the anthropogenic and climatic impacts on water
578 discharge and sediment load in the Pearl River (Zhujiang), China (1954-2009). *J. Hydrol.* 452-453, 190–
579 204. doi:10.1016/j.jhydrol.2012.05.064

580

581

582 Table 1 Variance and copula variance calculated for 4 discharge time series

583

584

	ANDE	COCH	MAXA	PLOC
<i>Var</i>	1.79	2.24	1.75	2.72
<i>Var_{cop}</i> [$\times 10^{-5}$]	3.01	1.64	5.39	1.27

585

586 Table 2 Covariance, correlation, copula covariance and copula correlation between 4 discharge data

587 (AN:Andernach, CO:Cochem, MA:Maxau, PL:Plochingen)

588

589

	AN-CO	AN-MA	AN-PL	CO-MA	CO-PL	MA-PL
<i>Cov</i>	1.68	1.60	1.33	1.38	1.31	1.41
<i>Cor</i>	0.84	0.90	0.60	0.70	0.53	0.64
<i>Cov_{cop}</i> [$\times 10^{-6}$]	4.90	3.40	3.39	7.16	9.90	5.47
<i>Cor_{cop}</i>	0.60	0.77	0.46	0.71	0.60	0.59

590

591 Table 3 Variance and copula variance calculated for API time series of 4 regions in the Baden-

592 Württemberg state of Germany

593

594

	C	SW	NW	NE
<i>Var</i>	1.70	1.66	1.72	1.78
<i>Var_{cop}</i> [$\times 10^{-6}$]	3.00	4.02	3.35	3.21

595

596

597 Table 4 Covariance, correlation, copula covariance and copula correlation between API time series from 4

598 regions in the Baden-Württemberg state of Germany

599

600

	C-SW	C-NW	C-NE	SW-NW	SW-NE	NW-NE
<i>Cov</i>	1.35	1.33	1.44	1.25	1.41	1.42
<i>Cor</i>	0.80	0.77	0.84	0.74	0.84	0.83
<i>Cov_{cop}</i> [$\times 10^{-7}$]	1.46	1.16	8.94	4.42	1.11	8.80
<i>Cor_{cop}</i>	0.36	0.29	0.29	0.09	0.26	0.24

601

Figure Captions

Figure 1 Locations of 7 discharge gauging stations in the Upper Rhine Region

Figure 2 Visualization of the functions which displays the contribution of a realization of (U_t, U_{t+k}) to *assymetry1* (left) and *assymetry2* (right)

Figure 3 Sketch of the transformation from sample hydrograph (left) to empirical copula (right): Scatterplot of ranks are calculated from two values separated by time lag $k = 1$ [days] in a discharge time series of Andernach where *rank correlation* = 0.9870, $A_1(k = 1) = -0.0002398$ and $A_2(k = 1) = -0.00011037$. The possible combinations of high and low values, which has large impacts on asymmetry, are numbered (1) low to high, (2) high to high (3) high to low (4) low to low. Negative contribution to *assymetry2* is drawn with red circle, positive contribution with blue circle.

Figure 4 Annual cycle of mean discharge after smoothing (left) and annual cycle of standard deviation after smoothing (right)

Figure 5 Discharge time series between 1950 and 1955 before applying normalization (upper left) and after applying normalization (upper right). The variation of *assymetry2* function calculated for entire time series before applying normalization (bottom left) and after applying normalization (bottom right) with 90% confidence intervals (grey) calculated for 100 realizations of Gaussian process (dashed line is $A_2(k)$ calculated for one of the realization of Gaussian process).

Figure 6 Relation between Asymmetry and catchment characteristics: minimum of *assymetry2* of discharge and catchment area (top), lag at minimum of *assymetry2* of discharge and catchment area (middle), minimum of *assymetry2* of discharge and lag at minimum of *assymetry2* of discharge (bottom)

Figure 7 Temporal change of minimum of *assymetry2* for 7 discharge records and confidence intervals calculated from the Gaussian process (90% confidence interval with grey color and 60% confidence interval with dark grey color) and one of its realizations (dashed line)

Figure 8 Moving average and standard deviation of the 7 daily discharge records for the window size $w = 3000$

Figure 9 Annual minimum and mean of aggregated daily temperature in the Baden-Württemberg state of Germany

Figure 10 Copula distances of discharge time series in moving time window: moving variance (top), distance type1 (middle) and distance type2 (bottom) with 80% confidence interval of Gaussian process and one of its realization (dashed line)

Figure 11 Copula distances of discharge time series in moving time window: moving covariance (top), moving correlation (second), distance type3 (third) and distance type4 (bottom)

Figure 12 Locations of the precipitation gauge stations within the Baden-Württemberg (Germany) indicated by coloured circles. Upper Neckar catchment is drawn with green area and the location of gauging station is drawn with a square

638 Figure 13 Copula distances of API time series in moving time window: moving variance (top), copula
639 distance type1 (middle) and copula distance type2 (bottom) where ‘C’ denotes central, ‘SW’ denotes
640 southwest, ‘NW’ denotes northwest and ‘NE’ denotes northeast part of Baden-Württemberg State of
641 Germany respectively with 80% confidence interval of Gaussian process and one of its realization (dashed
642 line).

643 Figure 14 Copula distances of API time series in moving time window: moving covariance (top), moving
644 correlation (second), distance type3 (third) and distance type4 (bottom)

645 Figure 15 Copula distance type3 (top) and type4 (bottom) between 4 discharge and 1 API time series
646 which is aggregated for all the daily precipitations depicted in Figure 12

647 Figure 16 Copula asymmetry and copula distances for 30 simulated and one observed discharge time series
648 at Plochingen between 1965 and 2000: minimum of asymmetry2 for the time lag $k = 2$ [days] (top), copula
649 distance type1 (middle), copula distance type2 (bottom)

650

651

652

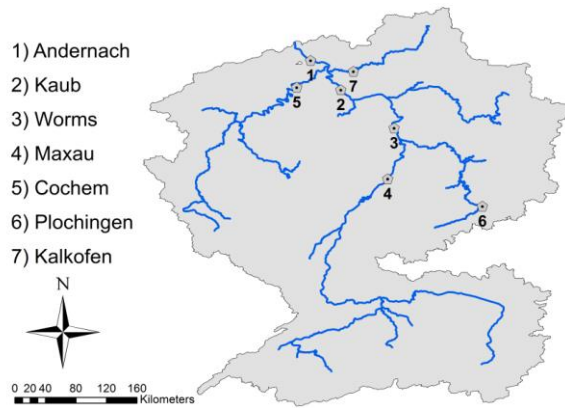


Figure 1 Locations of 7 discharge gauging stations in the Upper Rhine Region

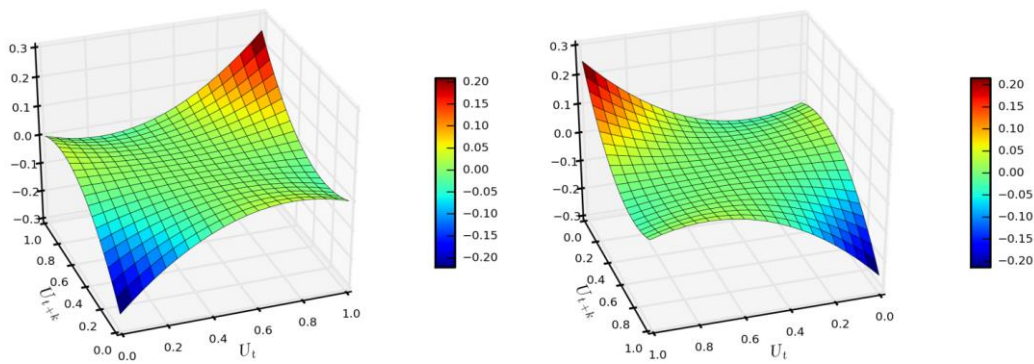


Figure 2 Visualization of the functions which displays the contribution of a realization of (U_t, U_{t+k}) to *asymmetry1* (left) and *asymmetry2* (right)

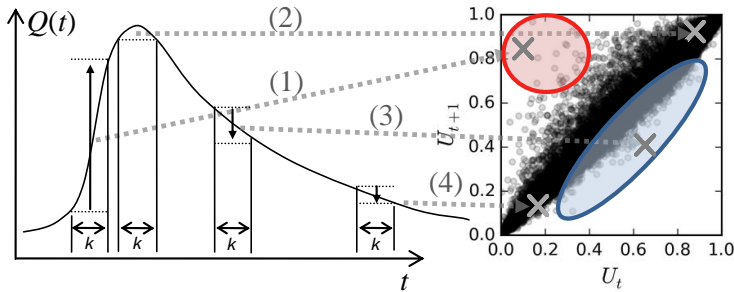


Figure 3 Sketch of the transformation of the values from sample hydrograph (left) to the points on scatterplot of ranks (right): empirical copula calculated from two values separated by time lag $k = 1$ [days] in a discharge time series of Andernach where $\text{rank correlation} = 0.9870$, $A_1(k = 1) = -0.0002398$ and $A_2(k = 1) = -0.00011037$. The possible combinations of high and low values, which has large impacts on asymmetry, are numbered: (1) low to high, (2) high to high, (3) high to low, (4) low to low. Negative contribution to asymmetry2 is drawn with red circle and positive contribution with blue oval.

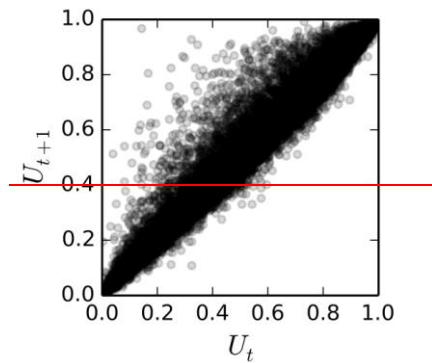


Figure 3 Scatterplot of ranks calculated from two values separated by time lag $k = 1$ [days] in a discharge time series of Andernach where $\text{rank correlation} = 0.9870$, $A_1(k = 1) = -0.0002398$ and $A_2(k = 1) = -0.00011037$

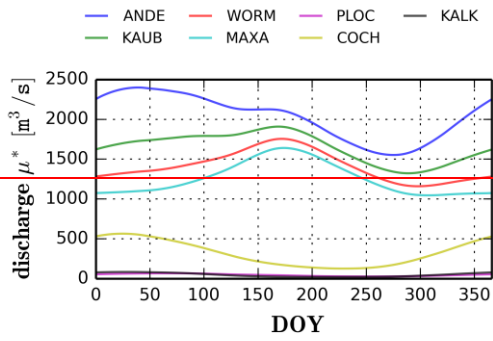
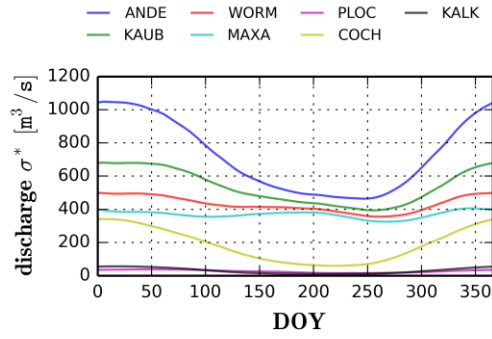
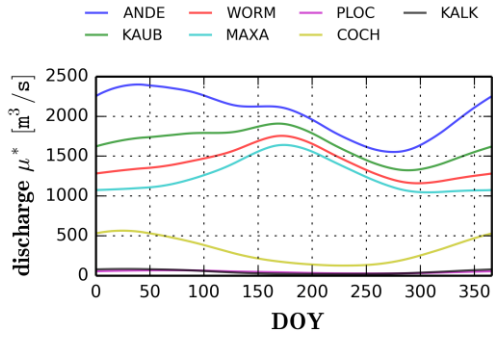
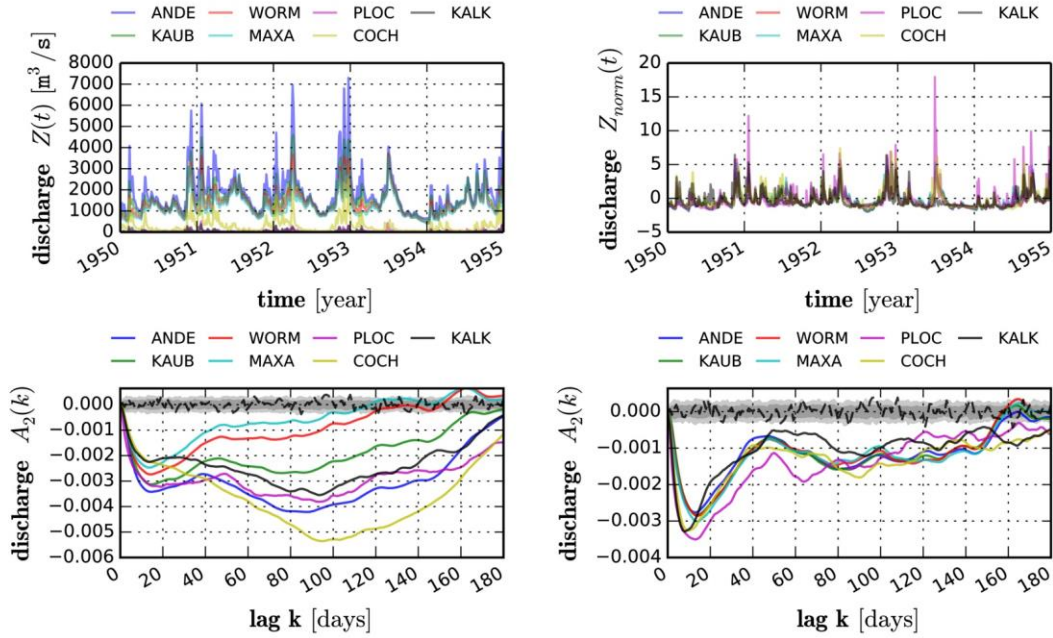
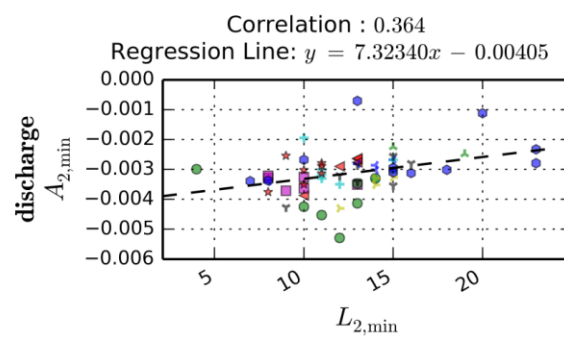
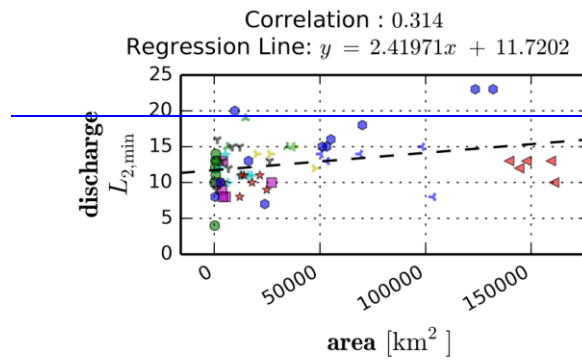
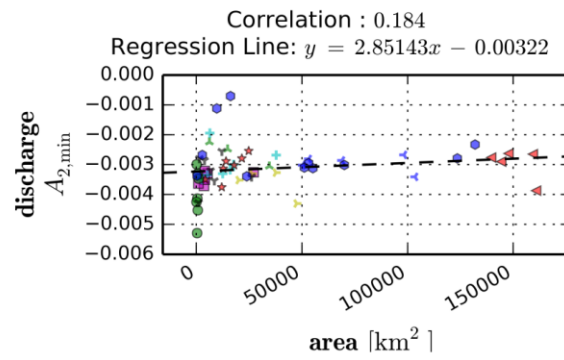


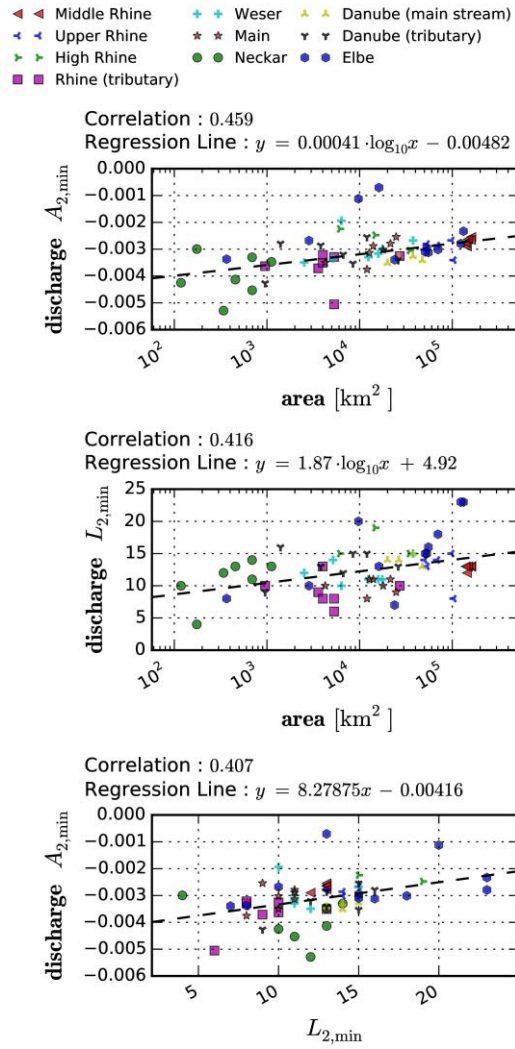
Figure 4 Annual cycle of mean discharge after smoothing (left) and annual cycle of standard deviation after smoothing (right)



676
677 Figure 5 Discharge time series between 1950 and 1955 before applying normalization (upper left) and after
678 applying normalization (upper right). The variation of asymmetry2 function calculated for entire time
679 series before applying normalization (bottom left) and after applying normalization (bottom right) with
680 90% confidence intervals (grey) calculated for 100 realizations of Gaussian process (dashed line is $A_2(k)$
681 calculated for one of the realization of Gaussian process).

- ▲ Middle Rhine
 + Weser
 ▼ Danube (main stream)
- ▲ Upper Rhine
 ★ Main
 ▼ Danube (tributary)
- ▲ High Rhine
 ● Neckar
 ● Elbe
- Rhine (tributary)



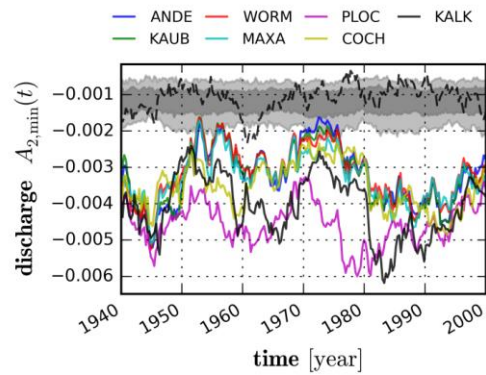


683

684 Figure 6 Relation between Asymmetry and catchment characteristics: minimum of asymmetry2 of
 685 discharge and catchment area (top), lag at minimum of asymmetry2 of discharge and catchment area
 686 (middle), minimum of asymmetry2 of discharge and lag at minimum of asymmetry2 of discharge (bottom)

687

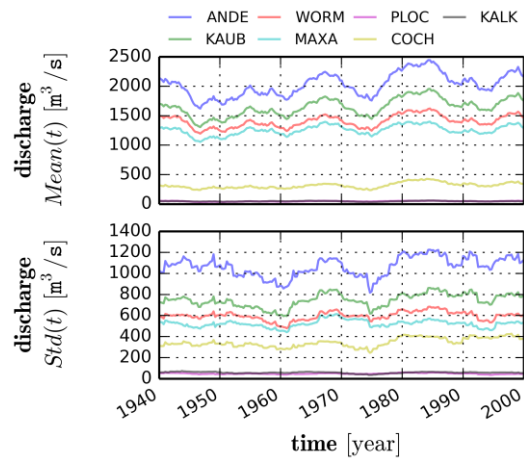
688



689

690 Figure 7 Temporal change of minimum of asymmetry2 for 7 discharge records and confidence intervals
691 calculated from the Gaussian process (90% confidence interval with grey color and 60% confidence
692 interval with dark grey color) and one of its realizations (dashed line)

693

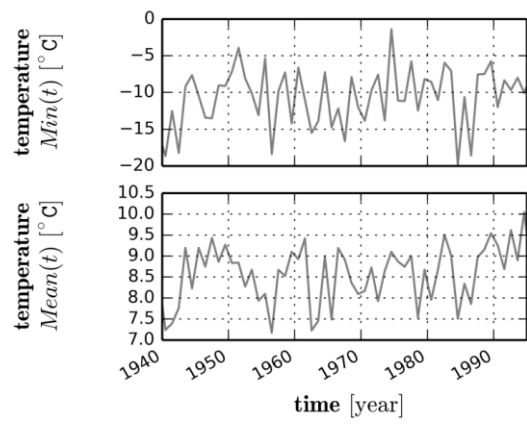


694

695 Figure 8 Moving average and standard deviation of the 7 daily discharge records for the window size $w =$
696 3000

697

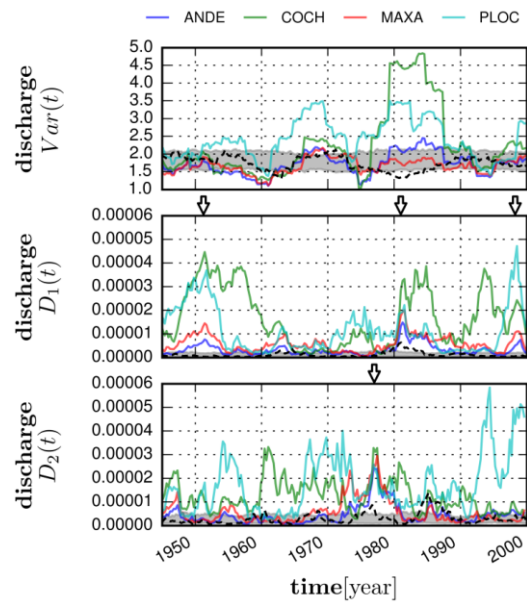
698



700

701 Figure 9 Annual minimum and mean of aggregated daily temperature in the Baden-Württemberg state of

702 Germany



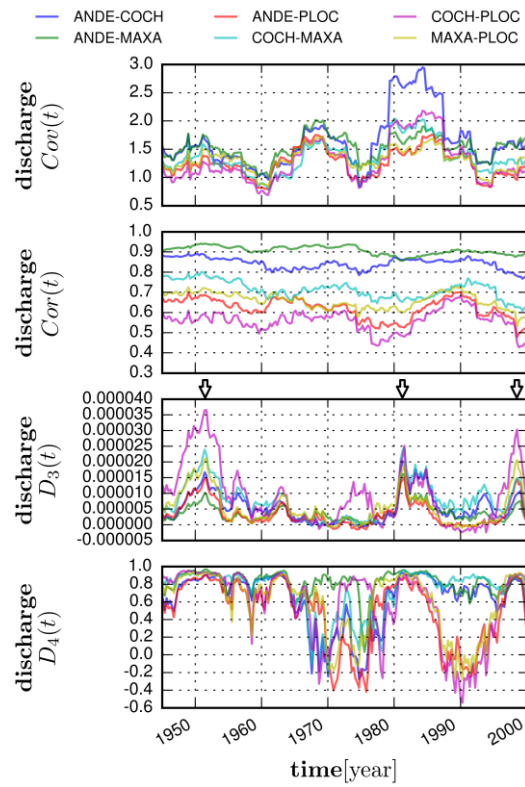
703

704 Figure 10 Copula distances of discharge time series in moving time window: moving variance (top),

705 distance type1 (middle) and distance type2 (bottom) with 80% confidence interval of Gaussian process and

706 one of its realization (dashed line)

707



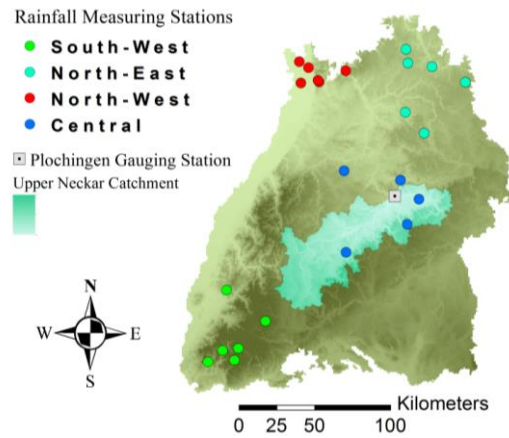
708

709 Figure 11 Copula distances of discharge time series in moving time window: moving covariance (top),

710 moving correlation (second), distance type3 (third) and distance type4 (bottom)

711

712



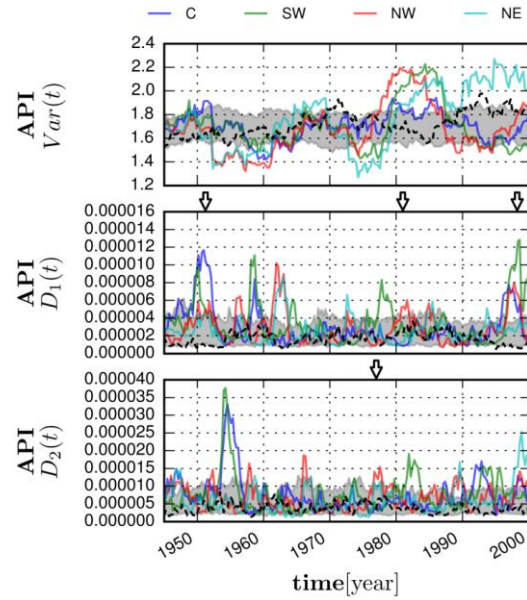
713

714 Figure 12 Locations of the precipitation gauge stations within the Baden-Württemberg (Germany)

715 indicated by coloured circles. Upper Neckar catchment is drawn with green area and the location of

716 gauging station is drawn with a square

717



718

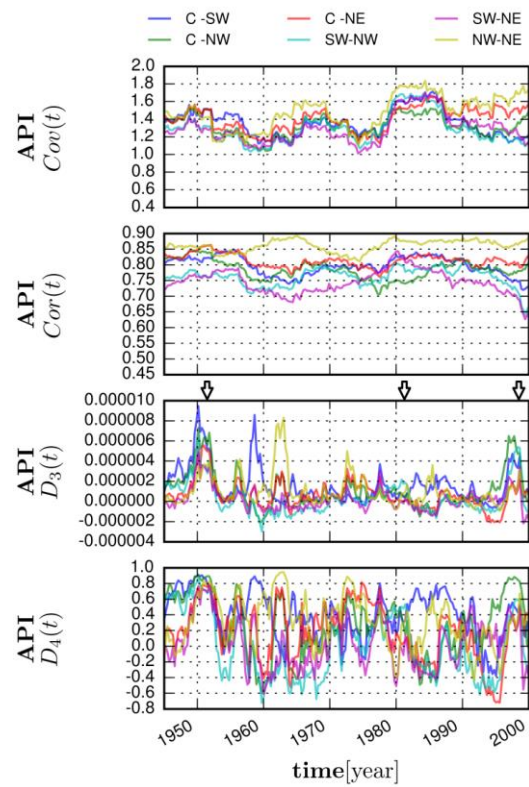
719 Figure 13 Copula distances of API time series in moving time window: moving variance (top), copula
 720 distance type1 (middle) and copula distance type2 (bottom) where ‘C’ denotes central, ‘SW’ denotes
 721 southwest, ‘NW’ denotes northwest and ‘NE’ denotes northeast part of Baden-Württemberg State of
 722 Germany respectively with 80% confidence interval of Gaussian process and one of its realization (dashed
 723 line).

724

725

726

727

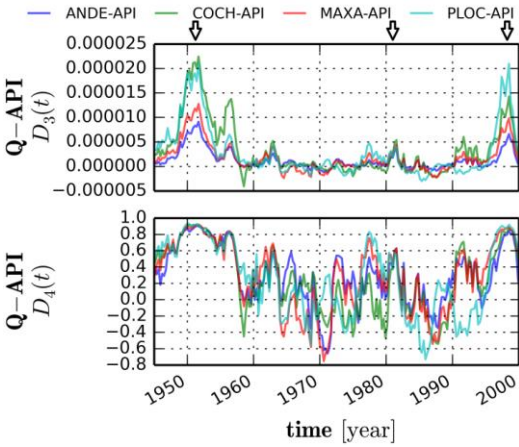


728

729 Figure 14 Copula distances of API time series in moving time window: moving
730 correlation (second), distance type3 (third) and distance type4 (bottom)

731

732

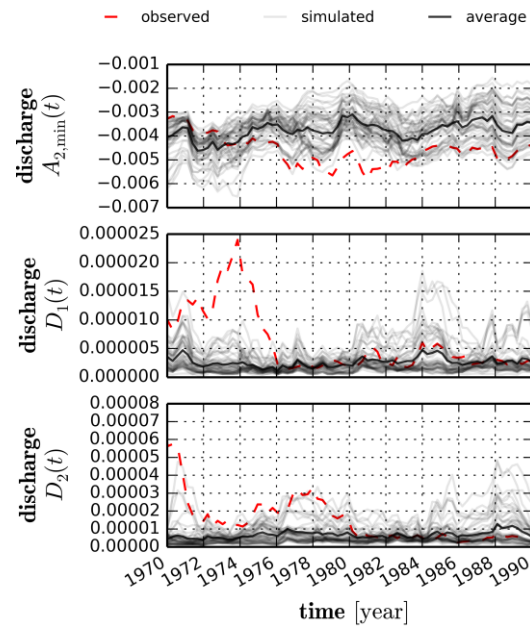


733

734 Figure 15 Copula distance type3 (top) and type4 (bottom) between 4 discharge and 1 API time series

735 which is aggregated for all the daily precipitations depicted in [Figure 12](#)~~Figure 12~~~~Figure 12~~

736



737

738 Figure 16 Copula asymmetry and copula distances for 30 simulated and one observed discharge time series
739 at Plochingen between 1965 and 2000: minimum of asymmetry2 for the time lag $k = 2$ [days] (top), copula
740 distance type1 (middle), copula distance type2 (bottom)

741

742

743

744